

## Preparation of drug-loaded PLGA-PEG nanoparticles by membrane-assisted nanoprecipitation

Airama Albisa<sup>1,2,3</sup>, Emma Piacentini<sup>3\*</sup>, Victor Sebastian<sup>1,4\*</sup>, Manuel Arruebo<sup>1,4</sup>, and Jesus Santamaria<sup>1,4</sup>, Lidietta Giorno<sup>3</sup>

<sup>1</sup>Department of Chemical & Environmental Engineering & Nanoscience Institute of Aragon (INA), University of Zaragoza, Mariano Esquillor edif. I+D, 50018 Zaragoza, Spain.

<sup>2</sup>Department of Environmental and Chemical Engineering, University of Calabria (DIATIC-UNICAL), via P. Bucci Cubo 45<sup>a</sup>, 87036 Rende (CS), Italy

<sup>3</sup>Institute on Membrane Technology, National Research Council, ITM-CNR, Via P. Bucci 17/C, 87036 Rende (CS), Italy

<sup>4</sup>CIBER de Bioingeniería, Biomateriales y Nanomedicina (CIBER-BBN), Centro de Investigación Biomédica en Red, C/Monforte de Lemos 3-5, Pabellón 11, 28029 Madrid, Spain

\* Corresponding Authors

Author Information:

Airama Albisa: Mariano Esquillor edif. I+D, 50018 Zaragoza. Spain, [airama.albisa@gmail.com](mailto:airama.albisa@gmail.com); [airama@unizar.es](mailto:airama@unizar.es)

\* Emma Piacentini: Via P. Bucci 17/C, 87036 Rende (CS), Italy, Tel: (+39) 0984 492134, [e.piacentini@itm.cnr.it](mailto:e.piacentini@itm.cnr.it)

\* Victor Sebastian: Mariano Esquillor edif. I+D, 50018 Zaragoza. Spain, Tel: (+34) 876555441, [victorse@unizar.es](mailto:victorse@unizar.es)

Manuel Arruebo: Mariano Esquillor edif. I+D, 50018 Zaragoza. Spain, (+34) 876 555437,  
[arruebom@unizar.es](mailto:arruebom@unizar.es)

Jesus Santamaria: Mariano Esquillor edif. I+D, 50018 Zaragoza. Spain, (+34) 976 1000 Ext. 1153,  
[jesus.santamaria@unizar.es](mailto:jesus.santamaria@unizar.es)

Lidietta Giorno: Via P. Bucci 17/C, 87036 Rende (CS), Italy, (+39) 0984 492050,  
[l.giorno@itm.cnr.it](mailto:l.giorno@itm.cnr.it)

## **Abstract**

**Purpose.** The aim of this work is to develop a scalable continuous system suitable for the formulation of polymeric nanoparticles using membrane-assisted nanoprecipitation. One of the hurdles to overcome in the use of nanostructured materials as drug delivery vectors is their availability at industrial scale. Innovation in process technology is required to translate laboratory production into mass production while preserving their desired nanoscale characteristics.

**Methods.** Membrane-assisted nanoprecipitation has been used for the production of Poly[(D,L lactide-co-glycolide)-co-poly ethylene glycol] diblock) (PLGA-PEG) nanoparticles using a pulsed back-and-forward flow arrangement. Tubular Shirasu porous glass membranes (SPG) with pore diameters of 1 and 0.2  $\mu\text{m}$  were used to control the mixing process during the nanoprecipitation reaction.

**Results.** The size of the resulting PLGA-PEG nanoparticles could be readily tuned in the range from 250 to 400 nm with high homogeneity (PDI lower than 0.2) by controlling the dispersed phase volume/continuous phase volume ratio. Dexamethasone was successfully encapsulated in a continuous process, achieving an encapsulation efficiency and drug loading efficiency of 50% and 5%, respectively. The dexamethasone was released from the nanoparticles following Fickian kinetics.

**Conclusions.** The method allowed to produce polymeric nanoparticles for drug delivery with a high productivity, reproducibility and easy scalability.

## **Keywords:**

Nanoprecipitation, Membrane emulsification, PLGA-PEG, Dexamethasone, Nanoparticles

## **Abbreviations**

**CP:** continuous phase

**DEX:** dexamethasone

**DLE:** drug loading efficiency

**DP:** dispersed phase

**EE:** encapsulation efficiency

**MANA:** membrane-assisted nanoprecipitation

**NPs:** nanoparticles

**NSBTR:** nanoprecipitation in a stirred batch-type reactor

**PDI:** polydispersity index

**PEG:** poly ethylene glycol

**PGA:** glycolic acids

**PLA:** lactic acid

**PLGA-PEG:** Poly[(D,L lactide-co-glycolide)-co-poly ethylene glycol] diblock

**SEM:** Scanning Electron Microscopy

## Introduction

Polymeric nanoparticles (NPs) are intensely investigated due to their high potential, particularly, for diagnosis and drug-delivery applications [1]. They can be degraded in vivo, either enzymatically or by hydrolysis or both, to produce biocompatible, toxicologically safe by-products which are further eliminated by the normal metabolic pathways [2]. However, only a few of the drug-loaded nanoparticle systems investigated are able to reach the market. Among the main reasons for this are the difficulties regarding the scale-up of the manufacturing process, regulation standards and failure in clinical trials [3–5].

PLGA (poly-d,l-lactide-co-glycolide) is a FDA-approved polymer, used for the preparation of biodegradable nanosystems [2,6]. The rate of drug release from PLGA nanoparticles can be tuned by modifying the relative amount between lactic (PLA) and glycolic acids (PGA) in the polymer composition [2]. The release rate increases as the proportion of lactic acid decreases, due to the hydrophilicity increase in the matrix. The fastest degradation is achieved with PLGA 50% (PLA/PGA) [2,7]. On the other hand, PEG (poly ethylene glycol) is a hydrophilic and inert polymer that provides a steric barrier on the surface of the nanoparticles and minimizes their protein binding (opsonization). Adding PEG is useful to prolong NPs circulation (avoiding a fast clearance by macrophages) and to decrease premature drug release. Because of this, several copolymers of PLGA with PEG have been synthesized, encapsulating a wide variety of therapeutic drugs [8].

Different production techniques (i.e. nanoprecipitation, emulsion/solvent diffusion, spray drying, salting-out, supercritical antisolvent precipitation, etc.) have been reported for the synthesis of PLGA-PEG nanoparticles [9–12]. Among them, nanoprecipitation is highly attractive due to the low energy input required. Generally, the nanoprecipitation process yields nanoparticles after mixing a solution of the polymer in an organic solvent (i.e., acetone), with a non-solvent (i.e., water), where the polymer is not soluble. Consequently, the resulting nanoparticles are quite sensitive to the mixing process and solvents miscibility. NPs are formed due to the nucleation of small aggregates of polymeric macromolecules, followed by the aggregation of the formed nuclei to

Con formato: Inglés (Reino Unido)

generate a stable polymer nanoassembly. The aggregation stage is suppressed as soon as colloidal stability is reached. [13]

The main challenge in polymeric NPs production by nanoprecipitation process is to achieve a fine control of the mixing processes. This is crucial in order to tune with good accuracy, the size and physicochemical properties of the nanoparticles [14,15]. Producing polymeric NPs by an approach that meets clinics requirements remains highly challenging: it requires an operator independent, scalable and size-adjustable synthesis [16]. Typically, multistep batch laboratory procedures are not suitable for large-scale production due to the low reproducibility between batches [3]. A compromise often has to be accepted between the high throughput rates required and the ability to control the desired nanoscale features. Consequently, new technologies are required to overcome these challenges and significantly accelerate the clinical translation of nanomedicines [3,16].

The use of nanoprecipitation methods at industrial scale is still hindered by the lack of a robust technique able to translate the results from laboratory scale to mass production. Only few studies deal with the design of a reliable scale up of NPs production by nanoprecipitation [17]. Typically, a continuous system like a “T mixer” is used for large scale production where the two phases diffuse into each other forming the NPs. The work of [18] is a good example of this approach. However, the results achieved by these authors showed differences in terms of drug loading and particle size at laboratory scale and at pilot scale due to the higher turbulence generated in the continuous pilot scale mode (responsible of the drug diffusion in the external aqueous phase before the polymer chains aggregated to form the NPs) [18]. Automatically controlled devices, such as Semi-Automated Nanoprecipitation-System and high-throughput dynamic light scattering have been advocated to enable a good control over processing parameters while following a high-throughput approach [13,17,19].

Membranes are being increasingly used as the system of choice for scaling up the production of emulsions and particles. Membrane emulsification, also combined with secondary solidification reactions, is a well-established technology with demonstrated scale-up capabilities [20–23].

Con formato: Inglés (Reino Unido)

However, the study of nanoprecipitation in combination with membrane processing (membrane-assisted nanoprecipitation or MANA) has opened a new window on the application of membrane science in the last years [24–28].

In the present work, the production of PLGA-PEG NPs by MANA has been investigated for the first time. Our aim is to develop a scalable continuous system suitable for the formulation of PLGA-PEG NPs using MANA. We have studied process development and drug release aspects that are essential regarding a potential clinic translation and industrial scale production. Dexamethasone has been selected as a model drug in view of its well-known properties as an anti-inflammatory and immunosuppressant corticosteroid widely used for the treatment of different pathologies including arthritis, allergy, joint pain, skin and eye disorders, leukemia, lymphoma, multiple myeloma, cancer-associated side effects, inflammation, and immune-system disorders. Being a hydrophobic drug, encapsulation is often proposed to increase its bioavailability [29]. In this work, we have evaluated the encapsulation efficiency and drug loading efficiency of dexamethasone in PLGA-PEG NPs as well as its delivery profile to unveil the release mechanism.

## 2. Materials and Methods

### 2.1. Materials

Poly[(D,L-lactide-co-glycolide)-co-PEG] diblock (PLGA-PEG) polymer: RESOMER Select 5050 DLG mPEG 5000 (Diblock PLGA (50:50) PEG (5kDa, 5%)) were purchased from EVONIK Industries AG. Pluronic F127 and Acetone were purchased from Sigma-Aldrich. Deionized water was used in all the experiments. All chemicals used were reagent grade.

### 2.2. Production of PLGA-PEG nanoparticles by membrane –assisted nanoprecipitation

A polymeric solution of PLGA-PEG (10 mg mL<sup>-1</sup>) in acetone was used as dispersed phase (DP) and Pluronic F127 in water (11.6 mg mL<sup>-1</sup>) was used as continuous phase (CP). For the study of

dexamethasone (DEX) encapsulation efficiency and release, the DP was modified by including DEX (PLGA-PEG at 10 mg mL<sup>-1</sup> and DEX at 1 mg mL<sup>-1</sup> in acetone)

The preparation of polymeric nanoparticles was carried out by using a Shirasu porous glass (SPG, Miyazaki, Japan) hydrophilic tubular membrane. Membranes with a pore size of 1 and 0.2 µm were tested. The effective membrane area was 31.3 cm<sup>2</sup>. The schematic figure of the membrane apparatus used for nanoparticles preparation is illustrated in Figure 1. A pump was used to inject the dispersed phase through the membrane pores. The continuous phase was pulsed back-and forward (pulsed cross-flow mode) at a fixed amplitude and frequency along the lumen side of the membrane by a programmable peristaltic pump (Digi-Staltic double-Y Masterflex® pump Micropump, model GJ-N23.JF1SAB1). The value of the amplitude was fixed at 4.7 10<sup>-2</sup> m and the frequency was modified in the range between 1.48 and 3.57 Hz. The maximum shear stress (τ<sub>max</sub>) [Pa] is a function of the amplitude (a) and the frequency (f) of the pulsed flow according to equation 1 [30]:

$$\text{Equation 1} \quad \tau_{\max} = 2 a (\pi f)^{\frac{3}{2}} (\mu_c \rho_c)^{\frac{1}{2}}$$

Where τ<sub>max</sub> is the shear stress (Pa), ~~a~~a is the amplitude, f is the frequency, μ<sub>c</sub> is the continuous phase viscosity (Pa s) and ρ<sub>c</sub> is the continuous phase density (kg m<sup>-3</sup>).

The disperse phase flux (J<sub>d</sub>) was determined by the volumetric flow, measuring the dispersed phase consumption from the graduated feed cylinder. J<sub>d</sub> (L h<sup>-1</sup> m<sup>-2</sup>) is given by the following equation 2:

$$\text{Equation 2} \quad J_d = Q_d / A$$

Where, Q<sub>d</sub> is the dispersed phase flow rate (L h<sup>-1</sup>) and A is the membrane area (m<sup>2</sup>). The dispersed phase flow rate was varied between 9.6 10<sup>-3</sup> and 6 L h<sup>-1</sup> that corresponds to a dispersed phase flux between 3 and 1917 Lh<sup>-1</sup>m<sup>-2</sup>. Polymeric NPs are formed after the controlled diffusion of the dispersed phase into the continuous phase (Figure 1-b).

Different ratios of dispersed phase volume /continuous phase volume (DP/CP) were tested in the range from 0.46-32 to 1.22. Dispersed phase/continuous phase (DP/CP) ratio was calculated using equation 3. The DP volume corresponds to the total volume of polymeric solution permeated trough



the membrane at time t while the CP volume was constant and equal to 50mL. As a result, the DP/CP ratios increased as a function of time

Equation 3 
$$\text{DP/CP ratio (t)} = \text{DP Volume (t)} / \text{CP Volume}$$

At the end of each experiment, the produced droplets were collected and left under the fume hood for 3 hours to allow acetone evaporation. The resulting particles were centrifuged at 2100 g for 10 min, and the pellet washed three times with Milli-Q water using the centrifuge. The supernatant collected after each centrifugation cycle was stored for further analysis and the pellet was lyophilized for 24h (0.01 bar, -40°C) using a LyoAlfa 10/15 lyophilizer from Telstar.

### 2.3. Production of PLGA-PEG nanoparticles by nanoprecipitation in stirred batch-type reactor

The nanoprecipitation process was carried out in a beaker (batch-type reactor) and mixing was produced by magnetic stirring (300 rpm) at room temperature. In this case, the dispersed phase was added into the continuous phase drop by drop. The composition of the dispersed and continuous phases was the same as the one used for conducting the experiments with the MANA process.

A 150 mL batch-type reactor was filled with 50 mL of CP and the DP volume was gradually added (from 16 mL to 55 mL) to obtain a DP /CP volumetric ratios from 0.32-32 to 1.422. This procedure reproduces the conditions used by using the membrane equipment. For each DP/CP volume ratio studied, the produced droplets were collected and left under the fume hood for 3 hours to allow acetone evaporation. The resulting particles were centrifuged at 2100 g for 10 min, and the pellet washed three times with Milli-Q water using the centrifuge. The supernatant collected after each centrifugation cycle and the pellet was lyophilized for 24h (0.01 bar, -40°C) using a LyoAlfa 10/15 lyophilizer from Telstar.

### 2.4. Particles characterization

#### 2.4.1. Particle analysis

Particle size and polydispersity (PDI) of the nanoparticles were measured by Dynamic light-scattering (ZetaSize NanoZS, Malvern Instrument). The software used to collect and analyse the data was ZetaSizer Software 7.1 from Malvern. The measurements were made at a controlled temperature of 25°C. The Z-average diameter (Z-Average) and the polydispersity index (PDI) were obtained from the autocorrelation function using a refractive index of 1.55.

Morphological analysis of the nanoparticles was carried out by Scanning Electron Microscopy (SEM, Inspect F50; FEI, Eindhoven, the Netherlands) at the LMA-INA-Universidad Zaragoza facilities operated at 10–15 kV. Purified-collected samples were stained by mixing 200 uL of nanoparticles colloid with 200uL of phosphotungstic acid solution (75 mg/mL) during 1.5 hours. The resulting dispersion was washed three times with Milli-Q water using a centrifuge. Finally, 10 uL of resulting nanoparticles suspension was added on a glass slide, dried in air, and sputtered with platinum.

#### **2.4.2 Encapsulation Efficiency and Drug Loading Efficiency**

The encapsulation efficiency (EE) and drug loading efficiency (DLE) were calculated using an indirect method. The particles were separated from the liquid using Centrifugal Ultrafiltration Devices (Vivaspin) from Sartorius Stedim. DEX concentration in supernatant was measured directly after the centrifugation using HPLC analysis. DEX encapsulated was calculated by mass balance.

HPLC analysis was performed at 40 °C, using a reversed-phase C18 column (2.6 µm, 50x4.6mm Phenomenex kinetex) and eluted isocratically with acetonitrile/water (50/50 v/v). The flow rate was fixed at 0.4 mL/min and detection was obtained by UV detection at 260 nm. The linear regression coefficient determined in the range 0.01–30 µg mL<sup>-1</sup> was 0.9993 (n=10).

The EE and DLE were calculated according to equations 4 and 5, respectively.

$$\text{Equation 4} \quad \text{EE} = (\text{DEX encap})/(\text{DEX total}) * 100$$

$$\text{Equation 5} \quad \text{DLE} = (\text{DEX encap})/(\text{PLGA-PEG total}) * 100$$

Where EE is encapsulation efficiency (%), *DEX encaps* is Dexamethasone mass encapsulated (mg) and it was calculated from the difference of the *DEX total* (the initial Dexamethasone mass in the dispersed phase (mg)) and the amount of Dexamethasone in supernatant solutions, collected after each cycle of centrifugation (water continuous phase and washing solutions). ~~*DEX total* is the Initial Dexamethasone mass in the dispersed phase (mg)~~; DLE is drug loading efficiency (%) and PLGA-PEG total is Initial PLGA-PEG mass in the dispersed phase (mg)

### 2.4.3. In vitro drug release study

About 10 mg of lyophilized dexamethasone-loaded nanoparticles were transferred to the dialyzer and suspended in 200  $\mu$ L of release media (0.1 M PBS pH 7.4) at 37°C. The dialyzer was then introduced into an eppendorf vial containing release media (1 mL), which was stirred at 100 rpm using a magnetic stir bar. Dexamethasone release was assessed by intermittently sampling the contents of the release media, the buffer was replaced with fresh solution after sampling. Drug content during the release study was evaluated by HPLC using the same method described above.

The release profiles were evaluated by fitting the experimental data to equations describing different kinetic release. Linear regression analyses of the experimental data obtained from in-vitro drug release studies were made for four different models: zero order, first order, Korsmeyer–Peppas and Higuchi. A description of the method is reported in supporting information S3.

## 3. Results and Discussion

This section is structured in two main parts. The first deals with the investigation of the effect of phases composition, fluid dynamic conditions (dispersed phase flux and wall shear stress) and membrane pore size on the particle size and particle size distribution of PLGA-PEG nanoparticles produced by membrane-assisted nanoprecipitation. The second part includes the evaluation of encapsulation efficiency (EE), drug loading efficiency (DLE) and in vitro release of

dexamethasone-loaded PLGA-PEG nanoparticles prepared by membrane-assisted nanoprecipitation.

### 3.1 Effect of phases composition

PLGA-PEG concentration was kept constant at  $10 \text{ mg ml}^{-1}$ , a sufficiently diluted concentration to result in polymer nucleation [31]. The amounts of PLGA-PEG, acetone and water were modified in order to identify the respective polymer, solvent and non-solvent amounts required to obtain stable colloidal formulations at the defined ouzo region [32]. The construction of “Ouzo diagram” represents a meaningful resource for nanoprecipitation. To the best of our knowledge, no data are available in the literature for the ternary system PLGA-PEG/Acetone/water. On the other hand, a ternary diagram for PLGA, acetone, and water (containing 0.1 wt % of poloxamer 188) system, at  $25^\circ\text{C}$ , was determined by Beck-Broichsitter et al [33]. This ouzo diagram has been used as a reference in the present work to select the respective polymer, solvent and non-solvent amounts that resulted in nanoparticles production by solvent displacement. This assumption was considered correct because the physicochemical properties of PLGA-PEG and PLGA are similar, and then both polymers are expected to show a similar behaviour in the same acetone/water ternary system [34]. Both solubility and interaction parameters (such as solvent-water and polymer-solvent interaction) are reported to influence the phase mixing of the nanoprecipitation process [34]. PLGA-PEG mass fraction ( $f_{\text{PLGA-PEG}}$ ) and solvent mass fraction ( $f_{\text{Acetone}}$ ) studied in the present work were plotted together with the data obtained from the literature for PLGA in the ternary system water/acetone. Three regions have been identified: one phase region, stable ouzo region and unstable ouzo region (Figure 2) [33] obtained at different DP/CP volumetric ratios while maintaining constant the PLGA-PEG amount. Four samples were considered representative of the nanoprecipitation process: sample 1 ( $f_{\text{acetone}}$ : 0.20;  $f_{\text{PLGA}}$ :  $2.5 \cdot 10^{-3}$ ; DP/CP ratio: 0.32); sample 2 ( $f_{\text{acetone}}$ : 0.35;  $f_{\text{PLGA}}$ :  $4.5 \cdot 10^{-3}$ ; DP/CP ratio: 0.70), sample 3 ( $f_{\text{acetone}}$ : 0.49;  $f_{\text{PLGA}}$ :  $6.1 \cdot 10^{-3}$ ; ratio DP/CP: 1.22) and sample 4 ( $f_{\text{acetone}}$ : 0.7;  $f_{\text{PLGA}}$ :  $9.7 \cdot 10^{-3}$ ; DP/CP ratio: 3). SEM images from samples 1-3 confirm the stability of the colloids

formed in the stable Ouzo region (Figure 2). Those nanoparticles were uniform ( $PDI = 0.17 \pm 0.05$ ) and the particle size varied from  $261 \pm 28$  nm to  $390 \pm 40$  nm. SEM images of the particles produced in the unstable ouzo region (sample 4) by nanoprecipitation, reveal the presence of a bimodal size distribution ( $PDI=0.5$ ) with one population of particles in the range of 300 nm and the other in the range of 1000 nm. These results are in agreement with some previous systems not based on PLGA-PEG [35], where the production of monodisperse nanoparticles or a bimodal distribution of particles (nanoparticles + microparticles) was dependant on the location of synthesis conditions in relation to the stable and unstable ouzo regions, respectively. Data obtained in this work indicate that the PLGA-PEG nanoparticles can be produced by nanoprecipitation in the same range of acetone/water relative volume ratio as those reported for PLGA, thus validating the use of the diagram in figure 2 for our system. A DP/CP ratio higher than 3 resulted in the production of microparticles in addition to nanoparticles as a result of an excess of dissolved polymer in water [33,35].

The influence of the relative volume DP/CP on particle size and polydispersity has been evaluated by two approaches: 1) pulsed cross-flow membrane-assisted method and 2) a conventional stirred batch-type method (Figure 3). In case of pulsed cross-flow MANA, an increase of nanoparticle size was observed in the range from 250 to 400 nm as a function of DP/CP volumetric ratio increase. On the other hand, the PLGA-PEG NPs produced by nanoprecipitation in the conventional batch type reactor were not affected by the DP/CP ratio and NPs with a diameter of 100 nm were produced throughout the range explored (Figure 3). The different trend can be explained by the different mixing at the micro-scale obtained by these production methods. Nanoprecipitation occurs in three stages: 1) a nucleus is formed by several unimers of polymer; 2) nuclei growth occurs through a diffusion-limited process by addition of more unimers and 3) the growth process ends as a result of the formation of polymer brush layer on the nanoparticle surface [13]. In MANA the polymer solution is continuously added into the non-solvent phase, and solvent/non-solvent mixing occurs at the pore level where the two phases are in contact. The rate of solvent exchange is very high due to the steep concentration gradient and the formation of nuclei start. As soon as acetone passes through

the membrane pores, it gradually diffuses in the water, changing the composition of the CP. After nuclei formation, growth continues over time as the dispersed phase continues to flow through the membrane pores to achieve the required DP/CP volumetric ratio however, the fast initial decrease of polymer concentration prevents further generation of nuclei. The remaining dissolved polymer gradually precipitates over the nuclei formed as the counter-diffusion of water and acetone lowers its solubility. The final particle size is a result of a process of particle growth over the nuclei initially formed, rather than forming new entities. In contrast, the solvent-non-solvent mixing is instantaneous in batch nanoprecipitation, where the reagents were mixed by the vortex generated during the magnetic stirring. In this case the intense agitation accelerates the water-acetone mixing. As a consequence, all the nuclei are formed instantaneously, leading to a fast depletion of the polymer. In this case, the phase of gradual counter-diffusion of water and acetone does not exist and growth ends abruptly as soon as the polymer in the immediate vicinity of the nuclei has been used up. The resulting nanoparticles mean size was not a function of the mass fraction of acetone added. This observation was supported by the experiments carried out in batch process by simulating the conditions used in membrane experiments, where a volume of acetone (DP) from 16 to 55 mL was added drop-by-drop, in 50 mL of water to reach the desired DP/CP volumetric ratio. In this case, similar results, in terms of particle size and PDI, were obtained in batch methodology by maintaining constant the DP volume varying the CP volume from 4.1 mL to 100 mL. These results were in agreement with previous works that also reported the lack of influence of DP/CP ratio on particles sizes when precipitation was carried out in a stirred batch reactor [34,36,37]. The different results on the influence of the relative amount of DP and CP on particle size in membrane and batch systems suggest that the main role of the membrane in nanoprecipitation is to govern the nuclei growing step by controlling the mixing of solvent with non-solvent at the pore level. A PDI lower than 0.2 was obtained in both membrane-assisted and batch nanoprecipitation. However, in MANA the growth process is characterized by the deposition of several polymer unimers on the same nucleus formed at nucleation stage [14,15,38]. This extends the growth phase and allows control of

Con formato: Inglés (Reino Unido)

Con formato: Inglés (Reino Unido)

the particle size. Consequently, it can be concluded that unlike batch processes, membrane-assisted nanoprecipitation is a versatile procedure that enables to tune the size of the polymeric nanoparticles by varying the DP/CP ratio, at a given range of shear stress.

### 3.2 Effect of dispersed phase flux

The effect of dispersed phase flow rate on particle size and particle-size distribution of PLGA-PEG nanoparticles has been investigated. Three different DP flow rates were tested: 0.8, 3.2 and 100 mL min<sup>-1</sup>, corresponding to a range of flux from 15.3 to 1917 L h<sup>-1</sup>m<sup>-2</sup> maintaining constant the shear stress in 2.8 Pa. Figure 4 reports Z-average and PDI of PLGA-PEG nanoparticles produced by pulsed cross-flow membrane-based process as a function of DP flux. This very wide range of flow rate values has been selected in order to investigate the suitability of MANA to control nanoparticles formation over a large interval of processing rates. The high-end values of DP flux are sufficiently high to make the process attractive for industrial production. The results indicate that, for a given DP/CP ratio, particle size was almost independent on dispersed phase flow rate, giving a p-value >0.05 (Figure S1 in Supporting Information). Z-average values of 250 and 224 nm were obtained in the range of flux investigated for DP/CP ratios of 0.32 and 0.83, respectively. In addition, the PDI was always lower than 0.2, indicating a high uniformity on the PLGA-PEG nanoparticles irrespective of the DP Flux (Figure S2 in Supporting Information). This is in contrast with the usual results when membrane emulsification processes are used for particles production: the droplet size increases linearly with the dispersed phase flow rate because a necking time is usually required before droplets detachment from the membrane surface. During this time, an additional amount of the dispersed phase flows into the forming droplet [39]. However, as discussed above, our results indicate that in membrane-assisted nanoprecipitation, the formation of nanoparticle nuclei is practically instantaneous. These fast kinetics are able to accommodate the increased throughput (and the decreased contact time) as the flow rates of DP and CP are increased.

Similar results were obtained in previous works [40,40]. On the contrary, Khayata et al. 2012

Con formato: Inglés (Reino Unido)

obtained that the greater pressure of DP phase used (and then DP flow rate), the greater was the mean size of nanocapsules because droplets coalescence occurred during droplets formation from the membrane pores, supposing a drop-by-drop mechanism for nanoprecipitation membrane-assisted as in conventional membrane emulsification [41]. To clarify the mechanism of NPs formation in MANA, we have evaluated the wettability of SPG membranes by the dispersed phase. Using PLGA-PEG in acetone at  $10 \text{ mg mL}^{-1}$  the membrane was immediately wetted by the polymer solution and an accurate measurement of the contact angle was not possible (Figure 5-A). Only when the polymer concentration was sufficiently high ( $100 \text{ mg mL}^{-1}$ ) a contact angle of  $130^\circ$  was measured (Figure 5B). Because the membrane is highly wetted by the DP, we can conclude that under the conditions used in MANA, particle formation is not a result of a drop-by-drop mechanism but it is a consequence of phases micromixing at the pore level. This is also consistent with the results obtained in the previous section regarding the effect of the DP/CP ratio.

From our results, membrane-assisted nanoprecipitation emerges as a promising technology for nanoparticles production at large scale as demonstrated by increasing the dispersed phase flux over two orders of magnitude. A flux of  $1917 \text{ L h}^{-1}\text{m}^{-2}$  (PLGA-PEG Mass Flux  $192 \text{ g h}^{-1}\text{m}^{-2}$ ) could be employed without modifying the control over particles size and size distribution. This is in contrast with the results found when attempting to scale up membrane emulsification processes, where the dispersed phase flux is strongly limited [42]. Membranes not wetted by the DP are usually required to obtain droplets with controlled size and size distribution, but the low dispersed phase flux obtained results in low productivity [43]. This limitation is overcome in case of membrane-assisted nanoprecipitation as shown above. Membrane emulsification is recognised as a suitable process for the purpose of large scale emulsions and particles production considering the scale-up ability of membranes [21,42,44,45]. The development of large-scale membrane emulsification processes can be assessed either through parallelisation or through increasing individual membrane surface area. In the present work, to prove that the upscaling of the process can also be assessed, further

**Con formato:** Fuente:  
(Predeterminado) Times New  
Roman, 12 pto



experiments were also carried by increasing the volume of the continuous phase vessel up to 6 times and a production rate of 160 mg h<sup>-1</sup> was reached.

Con formato: Superíndice

### 3.3 Effect of wall shear stress

The shear stress depends on the frequency and the amplitude of the pulsation along the lumen side of the membrane. Figure 6 reports Z-average and PDI of PLGA-PEG nanoparticles produced by pulsed cross-flow membrane-based process as a function of the shear stress. The experiments were carried out by keeping constant the amplitude of the pulsation while increasing the frequency. Three different shear stresses were used 1.12; 2.48 and 4.16 Pa. The Z-Average and PDI were found approximately constant as the shear stress was increased (Figure 6 and Figure S3-S4 in supplementary information). The same morphology was also observed for PLGA-PEG nanoparticles produced by using different shear stress value as shown in Figure 7. Similar results were reported in the production of PCL nanoparticles by Khayata et al. by using SPG membranes in a cross-flow membrane emulsification system [41]. In conventional membrane emulsification a decrease in terms of particles size is observed when the shear stress was increased [46,47][44,45].

Código de campo cambiado

Con formato: Fuente: (Predeterminado) Times New Roman, 12 pto, Inglés (Reino Unido)

Con formato: Fuente: (Predeterminado) +Cuerpo (Calibri), 11 pto

The different trend can be explained considering that in nanoprecipitation the appropriate mixing between solvent and antisolvent controls the particles production instead of the balance between the shear force, exerted on the forming droplet by the continuous phase, and the interfacial tension as in membrane emulsification. The range of value of the shear stress selected in the present work did not allow to improve the solvent-antisolvent mixing however PDI lower than 0.2 indicates high uniformity of PLG-PEG-nanoparticles produced.

### 3.4. Effect of membrane pore size

The effect of membrane pore size on the mean size of PLGA-PEG nanoparticles prepared by pulsed-cross flow MANA process is reported in Figure 8. The mean nanoparticle size increased by

increasing the membrane pore size, and the effect was more pronounced at low DP/CP ratio (0.32). The average particle size increased from 210 to 288 nm (37%) and from 261 to 300 nm (15%), when membranes with pore sizes of 0.2 and 1  $\mu\text{m}$  were used, respectively. Z-average values also show to be significantly influenced by the pore size of the membrane (p value < 0.05 Figure S5) while PDI values were not significantly influenced by the pore size of the membrane (p value > 0.05 Figure S6). Although the results show that in nanoprecipitation particle size is sensitive to the membrane pore size, it should be highlighted that the particle size did not varied linearly with the pore size, which is the general trend observed in membrane emulsification process. These findings are in agreement with the results obtained by Charcosset et al. and Othman et al. [24,25]. In conventional membrane emulsification, a linear relationship exists between the pore size of the membrane and the droplet size, and membranes with a mean pore size smaller than the target particle size are required. In contrast, the membrane-assisted nanoprecipitation technique enables the production of particles significantly smaller in size than the pore size of the membrane. The production of Polycaprolactone (PCL) nanoparticles by nanoprecipitation in the range of size between 100 to 300 nm was obtained by using membranes with the pore size in the range between 6 to 100 nm [24] and 20 to 40  $\mu\text{m}$  [25]. These results can be explained by considering that the contact area between solvent and antisolvent is higher in case of big-pore membranes. Nucleation is extremely fast in nanoprecipitation (as discussed in section 3.1 above), therefore nuclei are quickly formed, as soon as the DP comes into contact with the CP. In a small-pore membrane, the supply of polymer to the formed nuclei is slower, so the particle does not have time to grow much until it is entrained into the CP. Growth is limited to the sphere of diffusion around the nuclei. As the pore size increases, diffusion is faster and nuclei grow into larger particles before entrainment in the CP (Figure 8).

Con formato: Inglés (Reino Unido)

Con formato: Inglés (Reino Unido)

### 3.5 Reproducibility of nanoprecipitation membrane-assisted process

Figure 9 reports the reproducibility achieved in the production of nanoparticles prepared by pulsed-cross flow membrane-assisted nanoprecipitation technique. Once a manufacturing process has been developed and have a good performance, it is required to go further and study if the process is consistent “in control” or it is unpredictable “out of control” [48][46]. Control charts are an excellent tool to inspect the process performance and enable to measure, monitor and control the production process. These facts make the control charts being widely used in pharmaceutical and biopharmaceuticals manufacturing processes [48-50][46-48]. Control charts of nanoprecipitation membrane-assisted process (Z- Average and PDI) were performed using 6 lots with the following operative conditions: DP/CP ratio of 0.32, shear stress of 2.48 Pa and DP flux of 61.3 L h<sup>-1</sup>m<sup>-2</sup> control chart methodology was employed and media, upper control limit (UCL) and the lower control limit (LCL) was calculated (see Supporting Information). Figure 9-a, in which the Z-average is plotted against the different batches of nanoparticles produced, shows that there is no variability between the samples and all the range of measurements are fairly narrow and close to the mean (250 nm). On the other hand, the analysis of PDI variations between lots also confirms the reproducibility between lots, obtaining a narrow PDI variation (Figure 9-b).

### 3.6 Encapsulation efficiency (EE) and drug loading efficiency (DLE)

Figure 10 depicts the effect of DP/CP ratio on the dexamethasone encapsulation efficiency (EE) and drug loading efficiency (DLE) of PLGA-PEG nanoparticles produced by pulsed-cross flow MANA. DLE is highly relevant in drug delivery because achieving a high drug loading allows reducing the content of the carrier material [51][49]. However, in terms of productivity, EE has a relevant economic impact considering that drugs are usually the most expensive components of pharmaceutical formulations. Consequently, it is desirable to maximize both parameters, EE and DLE. According to the results obtained in this work, the EE decreases in the range from 52.3 % to 34 % as a function of the increase of DP/CP ratio. The same trend was obtained in case of DLE. These insights about the DC/CP influence are in agreement with previously reported data where a

**Código de campo cambiado**

**Con formato:** Fuente: (Predeterminado) Times New Roman, 12 pto, Inglés (Reino Unido)

**Con formato:** Fuente: (Predeterminado) +Cuerpo (Calibri), 11 pto

**Código de campo cambiado**

**Con formato:** Inglés (Reino Unido)

**Código de campo cambiado**

**Con formato:** Fuente: (Predeterminado) Times New Roman, 12 pto, Inglés (Reino Unido)

**Con formato:** Fuente: (Predeterminado) +Cuerpo (Calibri), 11 pto

variety of drugs were encapsulated in different polymers by nanoprecipitation procedure [34,52-54][34,50-52]. A large volume of the non-solvent phase (i.e., a low DP/CP ratio) provides a high concentration gradient of the organic solvent across the phase boundary, leading to fast solidification of the particles [55][53]. Conversely, at high DP/CP ratio, the diffusion of acetone is delayed by the presence of the acetone in water. In addition, the solubility of dexamethasone in the water phase is an important parameter determining the maximum amount of drug that can be dissolved in the external phase, during the solidification step. Dexamethasone is a hydrophobic drug with a water solubility of 0.1 mg mL<sup>-1</sup>. The diffusion of acetone out of particle together with the drug occurs during polymer precipitation and the partition between the organic and the aqueous phases continues until the equilibrium is reached, decreasing the entrapment into the nanoparticles [56][54]. Our results are in agreement with the data reported in literature by Campus et al. They obtained an EE of 48% for dexamethasone-loaded PLGA nanoparticles, using acetone as solvent and a DP/CP ratio of 0.25. [57][55].

### 3.7 Release studies from the drug loaded nanoparticles

In vitro release studies of dexamethasone from PLGA-PEG nanoparticles were carried out during 15 days. The delivery profile showed: 1) a low release of dexamethasone during the first 2 h (induction time) of the test that can be attributed to nonencapsulated drug or drug on the surface, 2) an increase of drug release for the following 4 days that can be attributed to drug diffusion through pores and 3) a constant release rate that could be related with the polymer degradation and a slow drug diffusion (Figure 11). The initial burst release is commonly observed for biodegradable polymeric systems, where a high percentage of the biomolecule is released [58][56]. Initial burst release is expected to increase for drugs with a higher solubility and also as the drug is located on the surface of the nanoparticles, where the diffusion paths are negligible. In this case the relatively low burst release observed is noteworthy since dexamethasone is not a highly hydrophobic drug, with a significant water solubility of 0.1 mg mL<sup>-1</sup>. For instance, in a previous work [59][57] with

**Código de campo cambiado**

**Con formato:** Inglés (Reino Unido)

**Con formato:** Fuente: (Predeterminado) Times New Roman, 12 pto, Inglés (Reino Unido)

**Con formato:** Fuente: (Predeterminado) +Cuerpo (Calibri), 11 pto, Inglés (Reino Unido)

**Código de campo cambiado**

**Código de campo cambiado**

**Con formato:** Fuente: (Predeterminado) Times New Roman, 12 pto, Inglés (Reino Unido)

**Con formato:** Fuente: (Predeterminado) +Cuerpo (Calibri), 11 pto

**Código de campo cambiado**

**Con formato:** Fuente: (Predeterminado) Times New Roman, 12 pto, Inglés (Reino Unido)

**Con formato:** Fuente: (Predeterminado) +Cuerpo (Calibri), 11 pto

**Código de campo cambiado**

**Con formato:** Fuente: (Predeterminado) Times New Roman, 12 pto, Inglés (Reino Unido)

**Con formato:** Fuente: (Predeterminado) +Cuerpo (Calibri), 11 pto

**Con formato:** Fuente: (Predeterminado) Times New Roman, 12 pto, Inglés (Reino Unido)

**Con formato:** Fuente: (Predeterminado) +Cuerpo (Calibri), 11 pto

**Código de campo cambiado**

dexamethasone-loaded PLGA nanoparticles, a burst release of 60% in the first two days was found. This indicates a good distribution of dexamethasone in the PLGA-PEG nanoparticles, and also points to the effectiveness of PEG to reduce burst release. The complete release of the drug in PLGA polymeric particles could require one month due to the polymer hydrolysis. However in this case release was performed during 15 days because this period is enough to study the kinetics of the system [2].

A variety of release models were selected and used to fit the experimental data. Table 1 summarizes the most important kinetic parameters for each model obtained from statistical data fitting: the release constant (K), release exponent (n), and regression coefficient ( $R^2$ ).

On the basis of best fit with the highest correlation value ( $R^2$ ), it is concluded that model that better fits the experimental data obtained from in vitro drug release studies is the Korsmeyer-Peppas model ( $R^2 = 0.97$ ). The magnitude of the release exponent  $n$  was found to be smaller than 0.5 (0.31), indicating that the mechanism of dexamethasone release from PLGA-PEG nanoparticles during 15 days preferentially followed a Fickian diffusion process. Fickian diffusional release occurs by the usual molecular diffusion of the drug due to a chemical potential gradient while non-Fickian predominates when there are also effects of swelling, erosion, degradation, stresses, structural changes and relaxation of the material [60,61][58,59]. The findings obtained are in agreement with literature, where Fickian diffusion was predominant at early times in PLGA-PEG systems. Vega et al [62][60], reported the cumulative in vitro release profile of flurbiprofen-loaded PLGA-PEG nanoparticles, achieving the best fitting with Korsmeyer-Peppas model ( $R^2 = 0.94$ , release exponent = 0.16). Assuming that Fickian diffusion is directing the dexamethasone release implies that PLGA-PEG nanoparticles were not substantially degraded during the release interval. In fact, after the release interval the amount of dexamethasone loaded in PLGA-PEG nanoparticles was higher than 40%. The initial release intervals in PLGAs based polymeric particles are normally associated to the Fickian transport and Non-Fickian is gradually predominant as the erosion and degradation phenomena are evident by the formation of new pores in the polymeric matrix. Higuchi

**Con formato:** Fuente: (Predeterminado) Times New Roman, 12 pto, Inglés (Reino Unido)

**Código de campo cambiado**

**Con formato:** Fuente: (Predeterminado) +Cuerpo (Calibri), 11 pto

**Código de campo cambiado**

**Con formato:** Fuente: (Predeterminado) Times New Roman, 12 pto, Inglés (Reino Unido)

**Con formato:** Fuente: (Predeterminado) +Cuerpo (Calibri), 11 pto

model, a Fickian model, was also evaluated to fit the experimental release data, but a correlation factor  $R = 0.87$  was obtained (Table 1). It implies that dexamethanose release from PLGA-PEG nanoparticles is not a pure diffusion process. This fact can be justified because the release analysis is usually made global, presenting always one transport type more predominant than the other [59][57].

#### 4. Conclusions

In this work, the efficiency of membrane-assisted nanoprecipitation (MANA) process to tune PLGA-PEG nanoparticles size with high producibility has been demonstrated. PLGA-PEG nanoparticle size in the range from 250 to 400 nm and with a PDI lower than 0.2 were continuously obtained. The main role of the membrane was to govern nuclei formation and subsequent growth into nanoparticles by controlling the mixing of solvent and non-solvent at the pore level. Particle size and particle size distribution have been demonstrated to be independent on the dispersed phase flux. High fluxes of  $1917 \text{ L h}^{-1}\text{m}^{-2}$  could be employed while maintaining control over particles size and size distribution, showing a high potential for large scale production.

The highest dexamethasone encapsulation efficiency (54 %) and drug loading (5.2 %) were achieved at the lower dispersed phase volume/continuous volume ratio, i.e., in the presence of a high concentration gradient of the solvent across the phase boundary, leading to fast solidification of the particles. The dexamethasone release from PLGA-PEG nanoparticles was found to preferentially follow a Fickian diffusion process. A comparatively low initial burst release was obtained.

In summary, MANA seems a highly promising alternative as a reproducible, productive and low-energy method for the continuous production of size-tuneable drug-loaded nanoparticles.

#### 5. Acknowledgements

Código de campo cambiado

Con formato: Fuente: (Predeterminado) Times New Roman, 12 pto, Inglés (Reino Unido)

Con formato: Fuente: (Predeterminado) +Cuerpo (Calibri), 11 pto

The People Program (CIG-Marie Curie Actions, REA grant agreement no. 321642) and the ERC Consolidator Grant program (ERC-2013-CoG-614715, NANOHEDONISM), the Government of Aragon and the European Social Fund are gratefully acknowledged. CIBER-BBN is an initiative funded by the VI National R&D&i Plan 2008–2011 financed by the Instituto de Salud Carlos III with the assistance of the European Regional Development Fund. Program Erasmus Mundus Doctorate in Membrane Engineering-EUDIME (2011-0014) is gratefully acknowledged. The authors acknowledge the European Union, FESR, MIUR, MSE for the financial support to the project PON Olio Più - PON01\_01545, within the framework PON Ricerca e Competitività 2007–2013.

## References

- [1. Luque-Michel E, Imbuluzqueta E, Sebastián V, Blanco-Prieto MJ. Clinical advances of nanocarrier-based cancer therapy and diagnostics. \*Expert Opin. Drug Deliv.\* 2016;1–18.](#)
- [2. Makadia HK, Siegel SJ. Poly Lactic-co-Glycolic Acid \(PLGA\) as Biodegradable Controlled Drug Delivery Carrier. \*Polymers.\* 2011;3:1377–97.](#)
- [3. Sebastian V, Arruebo M, Santamaria J. Reaction Engineering Strategies for the Production of Inorganic Nanomaterials. \*Small.\* 2014;10:835–53.](#)
- [4. Noorlander CW, Kooi MW, Oomen AG, Park MV, Vandebriel RJ, Geertsma RE. Horizon scan of nanomedicinal products. \*Nanomed.\* 2015;10:1599–608.](#)
- [5. Sainz V, Conriot J, Matos AI, Peres C, Zupančič E, Moura L, et al. Regulatory aspects on nanomedicines. \*Biochem. Biophys. Res. Commun.\* \[Internet\]. 2015 \[cited 2015 Nov 4\]; Available from: <http://linkinghub.elsevier.com/retrieve/pii/S0006291X15304137>](#)
- [6. Chan JM, Valencia PM, Zhang L, Langer R, Farokhzad OC. Polymeric Nanoparticles for Drug Delivery. In: Grobmyer SR, Moudgil BM, editors. \*Cancer Nanotechnol.\* \[Internet\]. Totowa, NJ: Humana Press; 2010 \[cited 2015 Feb 22\]. p. 163–75. Available from: \[http://link.springer.com/10.1007/978-1-60761-609-2\\\_11\]\(http://link.springer.com/10.1007/978-1-60761-609-2\_11\)](#)
- [7. Faisant N, Siepmann J, Benoit JP. PLGA-based microparticles: elucidation of mechanisms and a new, simple mathematical model quantifying drug release. \*Eur. J. Pharm. Sci.\* 2002;15:355–66.](#)
- [8. Xu Q, Ensign LM, Boylan NJ, Schön A, Gong X, Yang J-C, et al. Impact of Surface Polyethylene Glycol \(PEG\) Density on Biodegradable Nanoparticle Transport in Mucus \*ex Vivo\* and Distribution \*in Vivo\*. \*ACS Nano.\* 2015;9:9217–27.](#)
- [9. Ghahremankhani AA, Dorkoosh F, Dinarvand R. PLGA-PEG-PLGA Tri-Block Copolymers as In Situ Gel-Forming Peptide Delivery System: Effect of Formulation Properties on Peptide Release. \*Pharm. Dev. Technol.\* 2008;13:49–55.](#)
- [10. Avgoustakis K. Pegylated Poly\(Lactide\) and Poly\(Lactide-Co-Glycolide\) Nanoparticles: Preparation, Properties and Possible Applications in Drug Delivery. \*Curr. Drug Deliv.\* 2004;1:321–33.](#)
- [11. Vllasaliu D, Fowler R, Stolnik S. PEGylated nanomedicines: recent progress and remaining concerns. \*Expert Opin. Drug Deliv.\* 2014;11:139–54.](#)
- [12. Xu S, Yang F, Zhou X, Zhuang Y, Liu B, Mu Y, et al. Uniform PEGylated PLGA Microcapsules with Embedded Fe<sub>3</sub>O<sub>4</sub> Nanoparticles for US/MR Dual-Modality Imaging. \*ACS Appl. Mater. Interfaces.\* 2015;7:20460–8.](#)
- [13. Schubert S, Delaney, Jr JT, Schubert US. Nanoprecipitation and nanoformulation of polymers: from history to powerful possibilities beyond poly\(lactic acid\). \*Soft Matter.\* 2011;7:1581–8.](#)
- [14. Johnson BK, Prud'homme RK. Chemical processing and micromixing in confined impinging jets. \*AIChE J.\* 2003;49:2264–82.](#)
- [15. Johnson BK, Prud'homme RK. Mechanism for Rapid Self-Assembly of Block Copolymer Nanoparticles. \*Phys. Rev. Lett.\* \[Internet\]. 2003 \[cited 2015 Oct 6\];91. Available from: <http://link.aps.org/doi/10.1103/PhysRevLett.91.118302>](#)

**Con formato:** Bibliografía, Control de líneas viudas y huérfanas, Ajustar espacio entre texto latino y asiático, Ajustar espacio entre texto asiático y números

**Código de campo cambiado**

**Con formato:** Inglés (Reino Unido)



- [16. De Solorzano IO, Uson L, Larrea A, Miana M, Sebastian V, Arruebo M. Continuous synthesis of drug-loaded nanoparticles using microchannel emulsification and numerical modeling: Effect of passive mixing. \*Int. J. Nanomedicine\*. 2016;11:3397–416.](#)
- [17. Rietscher R, Thum C, Lehr C-M, Schneider M. Semi-Automated Nanoprecipitation-System—An Option for Operator Independent, Scalable and Size Adjustable Nanoparticle Synthesis. \*Pharm. Res\*. 2015;32:1859–63.](#)
- [18. Galindo-Rodríguez SA, Puel F, Briançon S, Allémann E, Doelker E, Fessi H. Comparative scale-up of three methods for producing ibuprofen-loaded nanoparticles. \*Eur. J. Pharm. Sci\*. 2005;25:357–67.](#)
- [19. Perevyazko IY, Delaney JT, Vollrath A, Pavlov GM, Schubert S, Schubert US. Examination and optimization of the self-assembly of biocompatible, polymeric nanoparticles by high-throughput nanoprecipitation. \*Soft Matter\*. 2011;7:5030.](#)
- [20. Imbrogno A, Piacentini E, Drioli E, Giorno L. Preparation of uniform poly-caprolactone Microparticles by membrane emulsification/solvent diffusion process. \*J. Membr. Sci\*. 2014;467:262–8.](#)
- [21. Piacentini E, Drioli E, Giorno L. Membrane emulsification technology: Twenty-five years of inventions and research through patent survey. \*J. Membr. Sci\*. 2014;468:410–22.](#)
- [22. Vladisavljević GT. Structured microparticles with tailored properties produced by membrane emulsification. \*Adv. Colloid Interface Sci\*. 2015;225:53–87.](#)
- [23. Piacentini E, Dragosavac M., Giorno L. Pharmaceutical Particles Design by Membrane Emulsification. \*Curr. Pharm. Des\*. 2016;in press.](#)
- [24. Charcosset C, Fessi H. Preparation of nanoparticles with a membrane contactor. \*J. Membr. Sci\*. 2005;266:115–20.](#)
- [25. Othman R, Vladisavljević GT, Shahmohamadi H, Nagy ZK, Holdich RG. Formation of size-tuneable biodegradable polymeric nanoparticles by solvent displacement method using micro-engineered membranes fabricated by laser drilling and electroforming. \*Chem. Eng. J.\* \[Internet\]. 2016 \[cited 2016 Jul 7\]; Available from: <http://linkinghub.elsevier.com/retrieve/pii/S1385894716309573>](#)
- [26. Laouini A, Charcosset C, Fessi H, Holdich RG, Vladisavljević GT. Preparation of liposomes: a novel application of microengineered membranes - investigation of the process parameters and application to the encapsulation of vitamin E. \*RSC Adv\*. 2013;3:4985.](#)
- [27. Laouini A, Koutroumanis KP, Charcosset C, Georgiadou S, Fessi H, Holdich RG, et al. pH-Sensitive Micelles for Targeted Drug Delivery Prepared Using a Novel Membrane Contactor Method. \*ACS Appl. Mater. Interfaces\*. 2013;5:8939–47.](#)
- [28. Limayem Blouza I, Charcosset C, Sfar S, Fessi H. Preparation and characterization of spironolactone-loaded nanocapsules for paediatric use. \*Int. J. Pharm\*. 2006;325:124–31.](#)
- [29. Soleimani G, Daryadel A, Ansari Moghadam A, Sharif MR. The Comparison of Oral and IM Dexamethasone Efficacy in Croup Treatment. \*J. Compr. Pediatr\*. 2013;4:175–8.](#)
- [30. Piacentini E, Drioli E, Giorno L. Pulsed back-and-forward cross-flow batch membrane emulsification with high productivity to obtain highly uniform and concentrate emulsions. \*J. Membr. Sci\*. 2014;453:119–25.](#)
- [31. Cheng J, Teply B, Sherifi I, Sung J, Luther G, Gu F, et al. Formulation of functionalized PLGA–PEG nanoparticles for in vivo targeted drug delivery. \*Biomaterials\*. 2007;28:869–76.](#)

Con formato: Inglés (Reino Unido)

Con formato: Inglés (Reino Unido)

- [32. Ganachaud F, Katz JL. Nanoparticles and Nanocapsules Created Using the Ouzo Effect: Spontaneous Emulsification as an Alternative to Ultrasonic and High-Shear Devices. \*ChemPhysChem\*. 2005;6:209–16.](#)
- [33. Beck-Broichsitter M, Nicolas J, Couvreur P. Solvent selection causes remarkable shifts of the “Ouzo region” for poly\(lactide-co-glycolide\) nanoparticles prepared by nanoprecipitation. \*Nanoscale\*. 2015;7:9215–21.](#)
- [34. Mora-Huertas CE, Fessi H, Elaissari A. Influence of process and formulation parameters on the formation of submicron particles by solvent displacement and emulsification–diffusion methods. \*Adv. Colloid Interface Sci\*. 2011;163:90–122.](#)
- [35. Aubry J, Ganachaud F, Cohen Addad J-P, Cabane B. Nanoprecipitation of Polymethylmethacrylate by Solvent Shifting:1. Boundaries. \*Langmuir\*. 2009;25:1970–9.](#)
- [36. Stainmesse S, Orecchioni A-M, Nakache E, Puisieux F, Fessi H. Formation and stabilization of a biodegradable polymeric colloidal suspension of nanoparticles. \*Colloid Polym. Sci\*. 1995;273:505–11.](#)
- [37. Beck-Broichsitter M, Rytting E, Lehardt T, Wang X, Kissel T. Preparation of nanoparticles by solvent displacement for drug delivery: A shift in the “ouzo region” upon drug loading. \*Eur. J. Pharm. Sci\*. 2010;41:244–53.](#)
- [38. Karnik R, Gu F, Basto P, Cannizzaro C, Dean L, Kyei-Manu W, et al. Microfluidic Platform for Controlled Synthesis of Polymeric Nanoparticles. \*Nano Lett\*. 2008;8:2906–12.](#)
- [39. Vladisavljevic GT. Integrated Membrane Processes for the Preparation of Emulsions, Particles and Bubbles. \*Integr. Membr. Syst. Process\*. 2015;79.](#)
- [40. Laouini A, Jaafar-Maalej C, Sfar S, Charcosset C, Fessi H. Liposome preparation using a hollow fiber membrane contactor—Application to spirinolactone encapsulation. \*Int. J. Pharm\*. 2011;415:53–61.](#)
- [41. Khayata N, Abdelwahed W, Chehna MF, Charcosset C, Fessi H. Preparation of vitamin E loaded nanocapsules by the nanoprecipitation method: From laboratory scale to large scale using a membrane contactor. \*Int. J. Pharm\*. 2012;423:419–27.](#)
- [42. Spyropoulos F, Lloyd DM, Hancocks RD, Pawlik AK. Advances in membrane emulsification. Part B: recent developments in modelling and scale-up approaches. \*J. Sci. Food Agric\*. 2014;94:628–38.](#)
- [43. Piacentini E, Imbrogno A, Drioli E, Giorno L. Membranes with tailored wettability properties for the generation of uniform emulsion droplets with high efficiency. \*J. Membr. Sci\*. 2014;459:96–103.](#)
- [44. Gijsbertsen-Abrahamse A. Status of cross-flow membrane emulsification and outlook for industrial application. \*J. Membr. Sci\*. 2004;230:149–59.](#)
- [45. Charcosset C. Preparation of emulsions and particles by membrane emulsification for the food processing industry. \*J. Food Eng\*. 2009;92:241–9.](#)
- [46. Piacentini E, Giorno L, Dragosavac MM, Vladisavljević GT, Holdich RG. Microencapsulation of oil droplets using cold water fish gelatine/gum arabic complex coacervation by membrane emulsification. \*Food Res. Int\*. 2013;53:362–72.](#)
- [47. Imbrogno A, Dragosavac M., Piacentini E, Vladisavljević GT, Holdich RG, Giorno L. Polycaprolactone multicore-matrix particle for the simultaneous encapsulation of hydrophilic and hydrophobic compounds produced by membrane emulsification and solvent diffusion processes. \*Colloids Surf. B Biointerfaces\*. 2015;135:116–25.](#)

Con formato: Inglés (Reino Unido)

48. Kahraman C, Yanik S, editors. *Intelligent Decision Making in Quality Management* [Internet]. Cham: Springer International Publishing; 2016 [cited 2016 Sep 14]. Available from: <http://link.springer.com/10.1007/978-3-319-24499-0>
49. Ermer J, Ploss H-J. Validation in pharmaceutical analysis. *J. Pharm. Biomed. Anal.* 2005;37:859–70.
50. Zhang L, editor. *Nonclinical Statistics for Pharmaceutical and Biotechnology Industries* [Internet]. Cham: Springer International Publishing; 2016 [cited 2016 Sep 14]. Available from: <http://link.springer.com/10.1007/978-3-319-23558-5>
51. Villaverde A, editor. *Nanoparticles in translational science and medicine*. Amsterdam: Elsevier, Acad. Press; 2011.
52. Chorny M, Fishbein I, Danenberg HD, Golomb G. Lipophilic drug loaded nanospheres prepared by nanoprecipitation: effect of formulation variables on size, drug recovery and release kinetics. *J. Controlled Release.* 2002;83:389–400.
53. Budhian A, Siegel SJ, Winey KI. Haloperidol-loaded PLGA nanoparticles: Systematic study of particle size and drug content. *Int. J. Pharm.* 2007;336:367–75.
54. Guhagarkar SA, Malshe VC, Devarajan PV. Nanoparticles of Polyethylene Sebacate: A New Biodegradable Polymer. *AAPS PharmSciTech.* 2009;10:935–42.
55. Dhakar R. FROM FORMULATION VARIABLES TO DRUG ENTRAPMENT EFFICIENCY OF MICROSPHERES: A TECHNICAL REVIEW. *J. Drug Deliv. Ther.* [Internet]. 2012;2. Available from: <http://jddtonline.info/index.php/jddt/article/view/160>
56. Govender T, Stolnik S, Garnett MC, Illum L, Davis SS. PLGA nanoparticles prepared by nanoprecipitation: drug loading and release studies of a water soluble drug. *J. Control. Release Off. J. Control. Release Soc.* 1999;57:171–85.
57. Campos IMF, Santos TM, Cunha GMF, Silva KMMN, Domingues RZ, da Silva Cunha Júnior A, et al. Preparation and release characteristics of dexamethasone acetate loaded organochlorine-free poly(lactide-co-glycolide) nanoparticles. *J. Appl. Polym. Sci.* 2014;131:n/a-n/a.
58. Ford Versypt AN, Pack DW, Braatz RD. Mathematical modeling of drug delivery from autocatalytically degradable PLGA microspheres — A review. *J. Controlled Release.* 2013;165:29–37.
59. Kim D-H, Martin DC. Sustained release of dexamethasone from hydrophilic matrices using PLGA nanoparticles for neural drug delivery. *Biomaterials.* 2006;27:3031–7.
60. Ritger PL, Peppas NA. A simple equation for description of solute release I. Fickian and non-fickian release from non-swellable devices in the form of slabs, spheres, cylinders or discs. *J. Controlled Release.* 1987;5:23–36.
61. Grassi M, Grassi G. Mathematical Modelling and Controlled Drug Delivery: Matrix Systems. *Curr. Drug Deliv.* 2005;2:97–116.
62. Vega E, Egea, Calpena, Espina, García. Role of hydroxypropyl- $\beta$ -cyclodextrin on freeze-dried and gamma-irradiated PLGA and PLGA-PEG diblock copolymer nanospheres for ophthalmic flurbiprofen delivery. *Int. J. Nanomedicine.* 2012;1357.
1. Luque Michel E, Imbuluzqueta E, Sebastián V, Blanco Prieto MJ. Clinical advances of nanocarrier based cancer therapy and diagnostics. *Expert Opin. Drug Deliv.* 2016;1–18.

2. Makadia HK, Siegel SJ. Poly Lactic co Glycolic Acid (PLGA) as Biodegradable Controlled Drug Delivery Carrier. *Polymers*. 2011;3:1377–97.
3. Sebastian V, Arruebo M, Santamaria J. Reaction Engineering Strategies for the Production of Inorganic Nanomaterials. *Small*. 2014;10:835–53.
4. Noorlander CW, Kooi MW, Oomen AG, Park MV, Vandebriel RJ, Geertsma RE. Horizon scan of nanomedicinal products. *Nanomed*. 2015;10:1599–608.
5. Sainz V, Conriot J, Matos AI, Peres C, Zupančič E, Moura L, et al. Regulatory aspects on nanomedicines. *Biochem. Biophys. Res. Commun.* [Internet]. 2015 [cited 2015 Nov 4]; Available from: <http://linkinghub.elsevier.com/retrieve/pii/S0006291X15304137>
6. Chan JM, Valencia PM, Zhang L, Langer R, Farokhzad OC. Polymeric Nanoparticles for Drug Delivery. In: Grobmyer SR, Moudgil BM, editors. *Cancer Nanotechnol.* [Internet]. Totowa, NJ: Humana Press; 2010 [cited 2015 Feb 22]. p. 163–75. Available from: [http://link.springer.com/10.1007/978-1-60761-609-2\\_11](http://link.springer.com/10.1007/978-1-60761-609-2_11)
7. Faisant N, Siepmann J, Benoit JP. PLGA-based microparticles: elucidation of mechanisms and a new, simple mathematical model quantifying drug release. *Eur. J. Pharm. Sci.* 2002;15:355–66.
8. Xu Q, Ensign LM, Boylan NJ, Schön A, Gong X, Yang J-C, et al. Impact of Surface Polyethylene Glycol (PEG) Density on Biodegradable Nanoparticle Transport in Mucus *ex Vivo* and Distribution *in Vivo*. *ACS Nano*. 2015;9:9217–27.
9. Ghahremankhani AA, Dorkoosh F, Dinarvand R. PLGA-PEG-PLGA Tri-Block Copolymers as In Situ Gel-Forming Peptide Delivery System: Effect of Formulation Properties on Peptide Release. *Pharm. Dev. Technol.* 2008;13:49–55.
10. Avgoustakis K. Pegylated Poly(Lactide) and Poly(Lactide Co Glycolide) Nanoparticles: Preparation, Properties and Possible Applications in Drug Delivery. *Curr. Drug Deliv.* 2004;1:321–33.
11. Villasaliu D, Fowler R, Stolnik S. PEGylated nanomedicines: recent progress and remaining concerns. *Expert Opin. Drug Deliv.* 2014;11:139–54.
12. Xu S, Yang F, Zhou X, Zhuang Y, Liu B, Mu Y, et al. Uniform PEGylated PLGA Microcapsules with Embedded Fe<sub>3</sub>O<sub>4</sub> Nanoparticles for US/MR Dual-Modality Imaging. *ACS Appl. Mater. Interfaces*. 2015;7:20460–8.
13. Schubert S, Delaney, Jr JT, Schubert US. Nanoprecipitation and nanoformulation of polymers: from history to powerful possibilities beyond poly(lactic acid). *Soft Matter*. 2011;7:1581–8.
14. Johnson BK, Prud'homme RK. Chemical processing and micromixing in confined impinging jets. *AIChE J*. 2003;49:2264–82.
15. Johnson BK, Prud'homme RK. Mechanism for Rapid Self-Assembly of Block Copolymer Nanoparticles. *Phys. Rev. Lett.* [Internet]. 2003 [cited 2015 Oct 6];91. Available from: <http://link.aps.org/doi/10.1103/PhysRevLett.91.118302>
16. De Solorzano IO, Uson L, Larrea A, Miana M, Sebastian V, Arruebo M. Continuous synthesis of drug-loaded nanoparticles using microchannel emulsification and numerical modeling: Effect of passive mixing. *Int. J. Nanomedicine*. 2016;11:3397–416.

17. Rietscher R, Thum C, Lehr C-M, Schneider M. Semi-Automated Nanoprecipitation System—An Option for Operator Independent, Scalable and Size Adjustable Nanoparticle Synthesis. *Pharm. Res.* 2015;32:1859–63.
18. Galindo-Rodríguez SA, Puel F, Briançon S, Allémann E, Doelker E, Fessi H. Comparative scale-up of three methods for producing ibuprofen-loaded nanoparticles. *Eur. J. Pharm. Sci.* 2005;25:357–67.
19. Perevyazko IV, Delaney JT, Vollrath A, Pavlov GM, Schubert S, Schubert US. Examination and optimization of the self assembly of biocompatible, polymeric nanoparticles by high throughput nanoprecipitation. *Soft Matter.* 2011;7:5030.
20. Imbrogno A, Piacentini E, Drioli E, Giorno L. Preparation of uniform poly-caprolactone Microparticles by membrane emulsification/solvent diffusion process. *J. Membr. Sci.* 2014;467:262–8.
21. Piacentini E, Drioli E, Giorno L. Membrane emulsification technology: Twenty five years of inventions and research through patent survey. *J. Membr. Sci.* 2014;468:410–22.
22. Vladisavljević GT. Structured microparticles with tailored properties produced by membrane emulsification. *Adv. Colloid Interface Sci.* 2015;225:53–87.
23. Piacentini E, Dragosavac M., Giorno L. Pharmaceutical Particles Design by Membrane Emulsification. *Curr. Pharm. Des.* 2016;in press.
24. Charcosset C, Fessi H. Preparation of nanoparticles with a membrane contactor. *J. Membr. Sci.* 2005;266:115–20.
25. Othman R, Vladisavljević GT, Shahmohamadi H, Nagy ZK, Holdich RG. Formation of size tuneable biodegradable polymeric nanoparticles by solvent displacement method using micro-engineered membranes fabricated by laser drilling and electroforming. *Chem. Eng. J.* [Internet]. 2016 [cited 2016 Jul 7]; Available from: <http://linkinghub.elsevier.com/retrieve/pii/S1385894716309573>
26. Laouini A, Charcosset C, Fessi H, Holdich RG, Vladisavljević GT. Preparation of liposomes: a novel application of microengineered membranes—investigation of the process parameters and application to the encapsulation of vitamin E. *RSC Adv.* 2013;3:4985.
27. Laouini A, Koutroumanis KP, Charcosset C, Georgiadou S, Fessi H, Holdich RG, et al. pH Sensitive Micelles for Targeted Drug Delivery Prepared Using a Novel Membrane Contactor Method. *ACS Appl. Mater. Interfaces.* 2013;5:8939–47.
28. Limayem-Blouza I, Charcosset C, Sfar S, Fessi H. Preparation and characterization of spironolactone-loaded nanocapsules for paediatric use. *Int. J. Pharm.* 2006;325:124–31.
29. Soleimani G, Daryadel A, Ansari Moghadam A, Sharif MR. The Comparison of Oral and IM Dexamethasone Efficacy in Croup Treatment. *J. Compr. Pediatr.* 2013;4:175–8.
30. Piacentini E, Drioli E, Giorno L. Pulsed back and forward cross-flow batch membrane emulsification with high productivity to obtain highly uniform and concentrate emulsions. *J. Membr. Sci.* 2014;453:119–25.
31. Cheng J, Teply B, Sherifi I, Sung J, Luther G, Gu F, et al. Formulation of functionalized PLGA-PEG nanoparticles for in vivo targeted drug delivery. *Biomaterials.* 2007;28:869–76.
32. Ganachaud F, Katz JL. Nanoparticles and Nanocapsules Created Using the Ouzo Effect: Spontaneous Emulsification as an Alternative to Ultrasonic and High Shear Devices. *ChemPhysChem.* 2005;6:209–16.

33. Beck-Broichsitter M, Nicolas J, Couvreur P. Solvent selection causes remarkable shifts of the “Ouzo region” for poly(lactide-co-glycolide) nanoparticles prepared by nanoprecipitation. *Nanoscale*. 2015;7:9215–21.
34. Mora-Huertas CE, Fessi H, Elaissari A. Influence of process and formulation parameters on the formation of submicron particles by solvent displacement and emulsification-diffusion methods. *Adv. Colloid Interface Sci.* 2011;163:90–122.
35. Aubry J, Ganachaud F, Cohen-Addad J-P, Cabane B. Nanoprecipitation of Polymethylmethacrylate by Solvent Shifting: 1. Boundaries. *Langmuir*. 2009;25:1970–9.
36. Stainmesse S, Orecchioni A-M, Nakache E, Puisieux F, Fessi H. Formation and stabilization of a biodegradable polymeric colloidal suspension of nanoparticles. *Colloid Polym. Sci.* 1995;273:505–11.
37. Beck-Broichsitter M, Rytting E, Lebbhardt T, Wang X, Kissel T. Preparation of nanoparticles by solvent displacement for drug delivery: A shift in the “ouzo region” upon drug loading. *Eur. J. Pharm. Sci.* 2010;41:244–53.
38. Karnik R, Gu F, Basto P, Cannizzaro C, Dean L, Kyei-Manu W, et al. Microfluidic Platform for Controlled Synthesis of Polymeric Nanoparticles. *Nano Lett.* 2008;8:2906–12.
39. Vladisavljević GT. Integrated Membrane Processes for the Preparation of Emulsions, Particles and Bubbles. *Integr. Membr. Syst. Process.* 2015;79.
40. Laouini A, Jaafar-Maalej C, Sfar S, Charcosset C, Fessi H. Liposome preparation using a hollow fiber membrane contactor—Application to spironolactone encapsulation. *Int. J. Pharm.* 2011;415:53–61.
41. Khayata N, Abdelwahed W, Chehna MF, Charcosset C, Fessi H. Preparation of vitamin E loaded nanocapsules by the nanoprecipitation method: From laboratory scale to large scale using a membrane contactor. *Int. J. Pharm.* 2012;423:419–27.
42. Spyropoulos F, Lloyd DM, Hancocks RD, Pawlik AK. Advances in membrane emulsification. Part B: recent developments in modelling and scale up approaches. *J. Sci. Food Agric.* 2014;94:628–38.
43. Piacentini E, Imbrogno A, Drioli E, Giorno L. Membranes with tailored wettability properties for the generation of uniform emulsion droplets with high efficiency. *J. Membr. Sci.* 2014;459:96–103.
44. Piacentini E, Giorno L, Dragosavac MM, Vladisavljević GT, Holdich RG. Microencapsulation of oil droplets using cold water fish gelatine/gum arabic complex coacervation by membrane emulsification. *Food Res. Int.* 2013;53:362–72.
45. Imbrogno A, Dragosavac M, Piacentini E, Vladisavljević GT, Holdich RG, Giorno L. Polycaprolactone multicore-matrix particle for the simultaneous encapsulation of hydrophilic and hydrophobic compounds produced by membrane emulsification and solvent diffusion processes. *Colloids Surf. B Biointerfaces*. 2015;135:116–25.
46. Kahraman C, Yanik S, editors. *Intelligent Decision Making in Quality Management [Internet]*. Cham: Springer International Publishing; 2016 [cited 2016 Sep 14]. Available from: <http://link.springer.com/10.1007/978-3-319-24499-0>
47. Ermer J, Ploss H J. Validation in pharmaceutical analysis. *J. Pharm. Biomed. Anal.* 2005;37:859–70.

48. Zhang L, editor. *Nonclinical Statistics for Pharmaceutical and Biotechnology Industries* [Internet]. Cham: Springer International Publishing; 2016 [cited 2016 Sep 14]. Available from: <http://link.springer.com/10.1007/978-3-319-23558-5>
49. Villaverde A, editor. *Nanoparticles in translational science and medicine*. Amsterdam: Elsevier, Acad. Press; 2011.
50. Chorny M, Fishbein I, Danenberg HD, Golomb G. Lipophilic drug-loaded nanospheres prepared by nanoprecipitation: effect of formulation variables on size, drug recovery and release kinetics. *J. Controlled Release*. 2002;83:389-400.
51. Budhian A, Siegel SJ, Winey KI. Haloperidol-loaded PLGA nanoparticles: Systematic study of particle size and drug content. *Int. J. Pharm.* 2007;336:367-75.
52. Guhagarkar SA, Malshe VC, Devarajan PV. Nanoparticles of Polyethylene Sebacate: A New Biodegradable Polymer. *AAPS PharmSciTech*. 2009;10:935-42.
53. Dhakar R. FROM FORMULATION VARIABLES TO DRUG ENTRAPMENT EFFICIENCY OF MICROSPHERES: A TECHNICAL REVIEW. *J. Drug Deliv. Ther.* [Internet]. 2012;2. Available from: <http://jddtonline.info/index.php/jddt/article/view/160>
54. Govender T, Stolnik S, Garnett MC, Illum L, Davis SS. PLGA nanoparticles prepared by nanoprecipitation: drug loading and release studies of a water soluble drug. *J. Control. Release Off. J. Control. Release Soc.* 1999;57:171-85.
55. Campos IMF, Santos TM, Cunha GMF, Silva KMMN, Domingues RZ, da Silva Cunha Júnior A, et al. Preparation and release characteristics of dexamethasone acetate loaded organochlorine-free poly(lactide-co-glycolide) nanoparticles. *J. Appl. Polym. Sci.* 2014;131:n/a-n/a.
56. Ford Versypt AN, Pack DW, Braatz RD. Mathematical modeling of drug delivery from autocatalytically degradable PLGA microspheres — A review. *J. Controlled Release*. 2013;165:29-37.
57. Kim D H, Martin DC. Sustained release of dexamethasone from hydrophilic matrices using PLGA nanoparticles for neural drug delivery. *Biomaterials*. 2006;27:3031-7.
58. Ritger PL, Peppas NA. A simple equation for description of solute release I. Fickian and non-fickian release from non-swellable devices in the form of slabs, spheres, cylinders or discs. *J. Controlled Release*. 1987;5:23-36.
59. Grassi M, Grassi G. Mathematical Modelling and Controlled Drug Delivery: Matrix Systems. *Curr. Drug Deliv.* 2005;2:97-116.
60. Vega E, Egea, Calpena, Espina, García. Role of hydroxypropyl- $\beta$ -cyclodextrin on freeze-dried and gamma-irradiated PLGA and PLGA-PEG diblock copolymer nanospheres for ophthalmic flurbiprofen delivery. *Int. J. Nanomedicine*. 2012;1357.

Con formato: Español (Español - alfab. tradicional)

## Legend to Figures

- Figure 1. a) Membrane-assisted nanoprecipitation set-up. b) Schematic representation of nanoparticles production by nanoprecipitation at the membrane level (green colour refers to the polymer dissolved in the solvent, yellow colour refers to the antisolvent).
- Figure 2. Location of the experimental points obtained in the present study for PLGA-PEG polymer (in red color) in the Ouzo diagram obtained by Beck-Broichsitter et al. (2015). SEM images of nanoparticles produced by nanoprecipitation membrane-assisted. Sample 1 (DP/CP ratio: 0.32). Sample 2 (DP/CP ratio: 0.70). Sample 3 (DP/CP ratio: 1.22). Sample 4 (DP/CP ratio: 3).
- Figure 3: Influence of DP/CP ratio on PLGA-PEG nanoparticles produced by using membrane-assisted nanoprecipitation approach (MANA) and nanoprecipitation in a stirred batch-type reactor (NSBTR) A) PLGA-PEG nanoparticles Z-Average; B) PLGA-PEG nanoparticles polydispersity index (PDI)
- Figure 4. The effect of dispersed phase flux on nanoparticle size and particle-size distribution of PLGA-PEG nanoparticles produced by membrane-assisted nanoprecipitation (Shear stress: 2.8 Pa).
- Figure 5. Contact angles of PLGA-PEG in acetone on SPG hydrophilic membrane A) PLGA-PEG 10 mg mL<sup>-1</sup> B) PLGA-PEG 100 mg mL<sup>-1</sup>
- Figure 6. Influence of wall shear stress on nanoparticle size and particle-size distribution of PLGA-PEG nanoparticles produced by membrane-assisted nanoprecipitation (DP flux: 61.3L h<sup>-1</sup>m<sup>-2</sup>; DP/CP ratio: 0.32).
- Figure 7. SEM images of PLGA-PEG nanoparticles produced by membrane-assisted nanoprecipitation at different shear stress values: A) 1.12 Pa B) 4.16 Pa.
- Figure 8. Influence of membrane pore size on nanoparticle size and particle size distribution of PLGA-PEG nanoparticles produced by membrane-assisted nanoprecipitation.



- Figure 9: Control Chart of 6 nanoparticles lots produced by nanoprecipitation membrane-assisted process (operating conditions: DP/CP ratio of 0.32, shear stress of 2.48 Pa and DP flux of  $61.3 \text{ L h}^{-1}\text{m}^{-2}$ ): A) Z-Average B) PDI
- Figure 10. Influence of DP/CP ratio on Encapsulation efficiency and Drug Loading of Dexamethasone encapsulated in PLGA-PEG nanoparticles produced by membrane-assisted nanoprecipitation.
- Figure 11. Dexamethasone release from PLGA-PEG nanoparticles produced by membrane-assisted nanoprecipitation.

#### **Tables Captions**

Table 1. Interpretation of  $R^2$  values and rate constants of dexamethasone release kinetics of PLGA-PEG nanoparticles

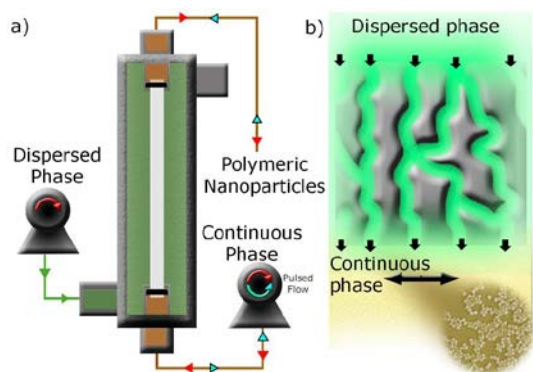


Figure 1. a) Membrane-assisted nanoprecipitation set-up. b) Schematic representation of nanoparticles production by nanoprecipitation at the membrane level (green colour refers to the polymer dissolved in the solvent, yellow colour refers to the antisolvent).

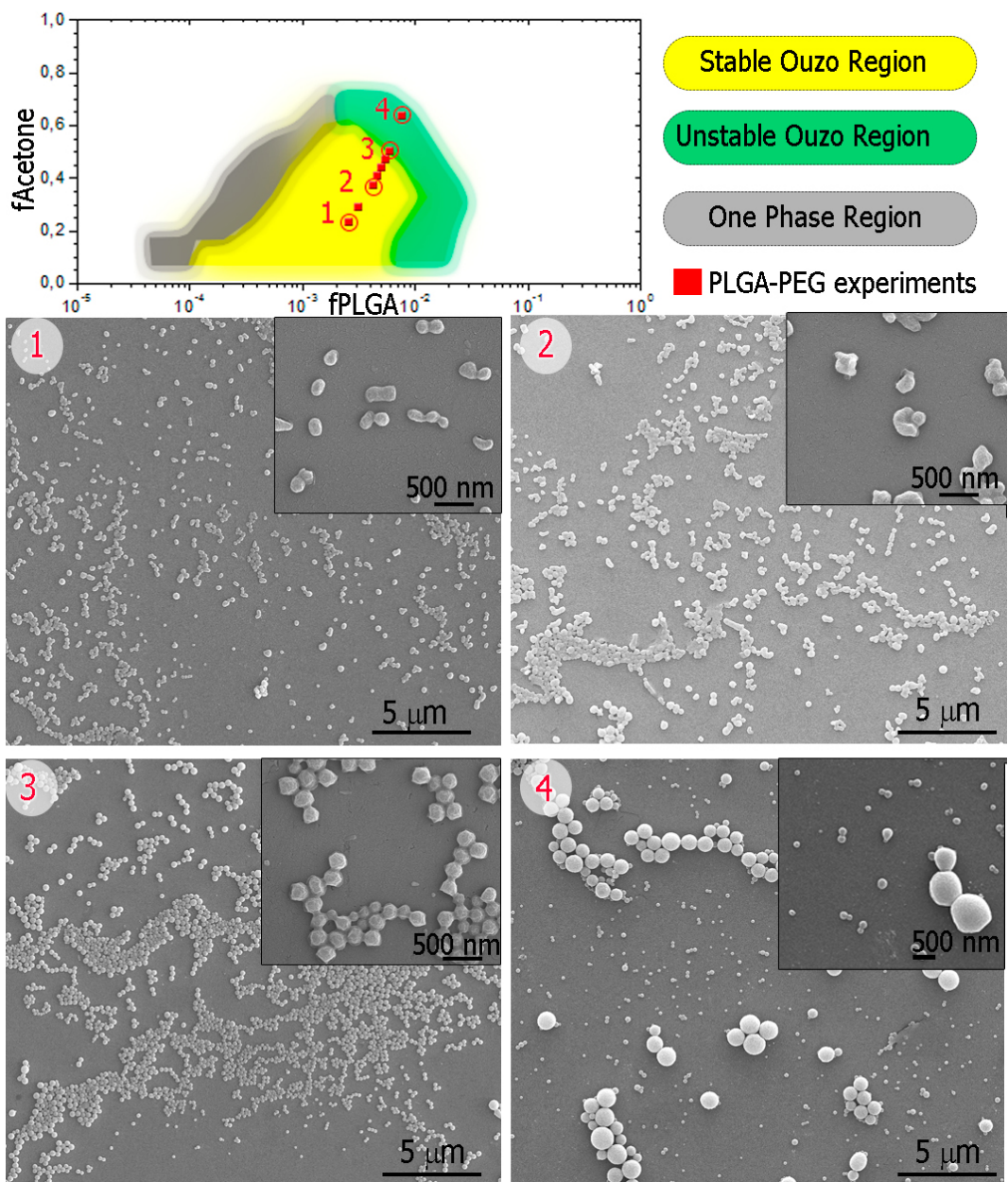


Figure 2. Location of the experimental points obtained in the present study for PLGA-PEG polymer (in red color) in the Ouzo diagram obtained by Beck-Broichsitter et al. (2015). SEM images of nanoparticles produced by nanoprecipitation membrane-assisted. Sample 1 (DP/CP ratio: 0.32). Sample 2 (DP/CP ratio: 0.70). Sample 3 (ratio DP/CP: 1.22). Sample 4 (DP/CP ratio: 3).

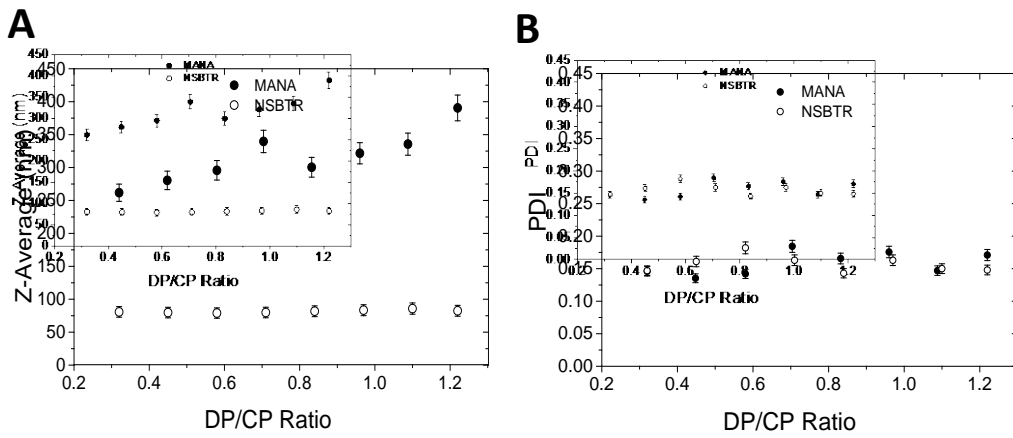


Figure 3: Influence of DP/CP ratio on PLGA-PEG nanoparticles produced by using membrane-assisted nanoprecipitation approach (MANA) and nanoprecipitation in a stirred batch-type reactor (NSBTR) A) PLGA-PEG nanoparticles Z-Average; B) PLGA-PEG nanoparticles polydispersity index (PDI)

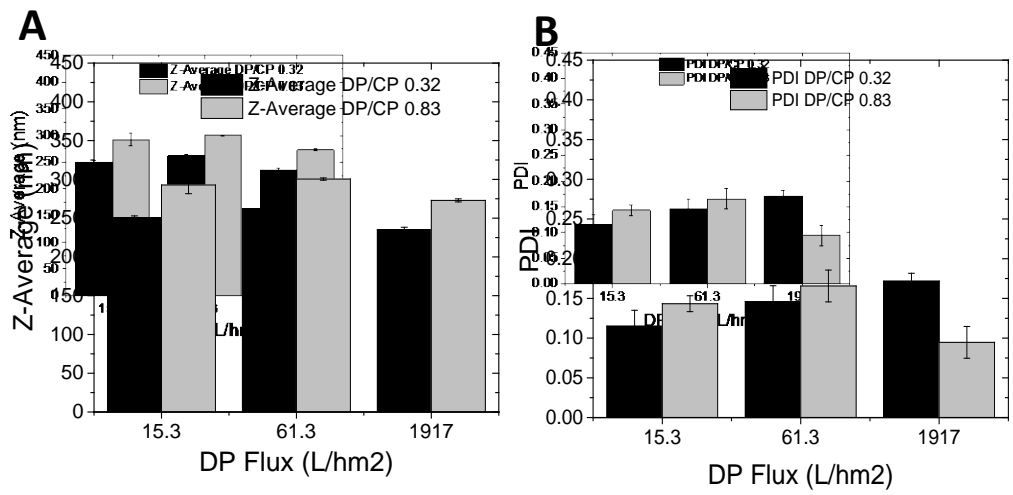


Figure 4. The effect of dispersed phase flux on nanoparticle size and particle-size distribution of PLGA-PEG nanoparticles produced by membrane-assisted nanoprecipitation (Shear stress: 2.8 Pa).

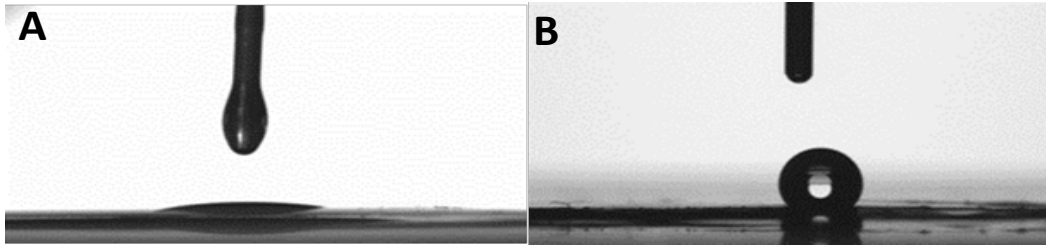


Figure 5. Contact angles of PLGA-PEG in acetone on SPG hydrophilic membrane A) PLGA-PEG 10 mg mL<sup>-1</sup> B) PLGA-PEG 100 mg mL<sup>-1</sup>

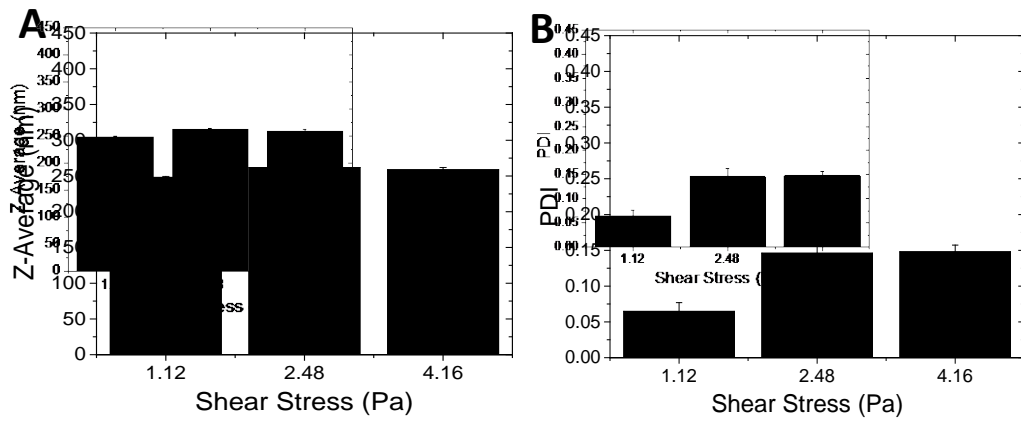


Figure 6. Influence of wall shear stress on nanoparticle size and particle-size distribution of PLGA-PEG nanoparticles produced by membrane-assisted nanoprecipitation (DP flux:  $61.3 \text{ L h}^{-1}\text{m}^{-2}$ ; DP/CP ratio: 0.32).

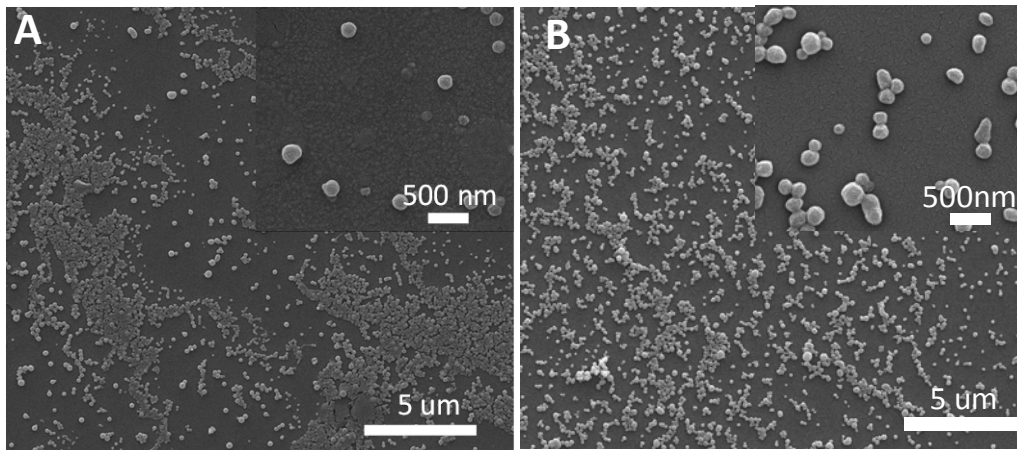


Figure 7. SEM images of PLGA-PEG nanoparticles produced by membrane-assisted nanoprecipitation at different shear stress values: A) 1.12 Pa B) 4.16 Pa.



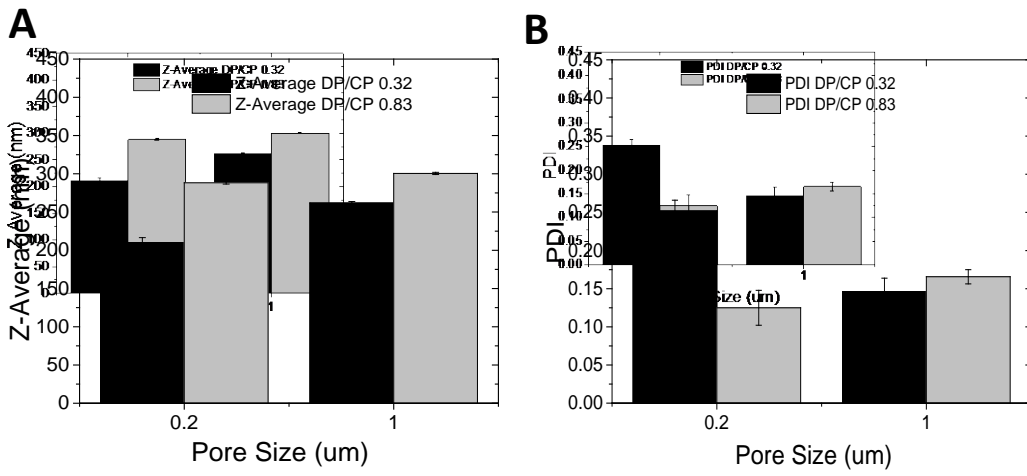


Figure 8. Influence of membrane pore size on nanoparticle size and particle size distribution of PLGA-PEG nanoparticles produced by membrane-assisted nanoprecipitation.

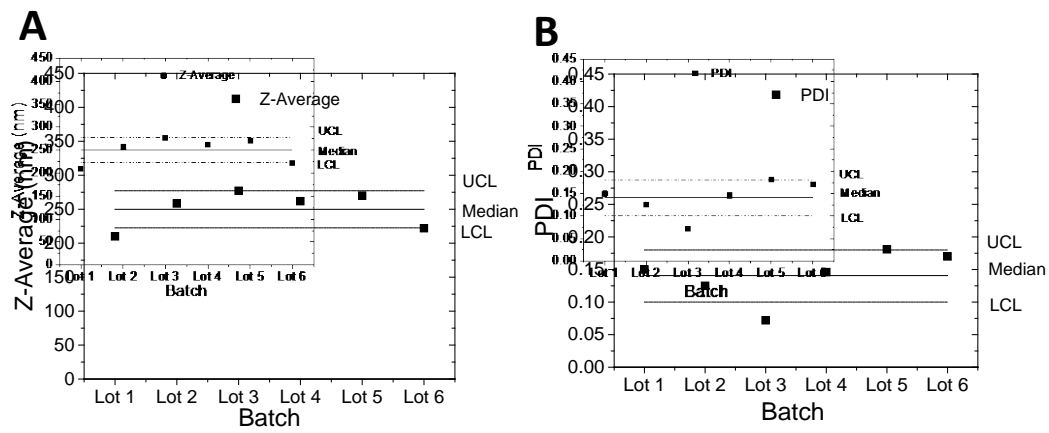
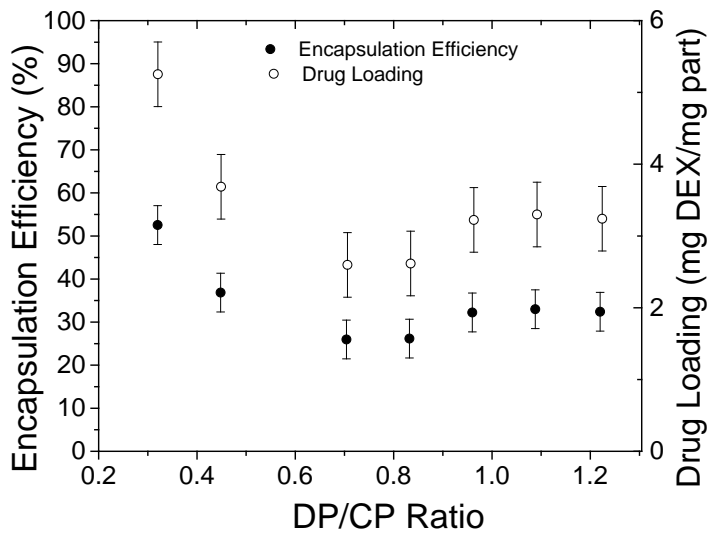


Figure 9: Control Chart of 6 nanoparticles lots produced by nanoprecipitation membrane-assisted process (operating conditions: DP/CP ratio of 0.32, shear stress of 2.48 Pa and DP flux of 61.3 L h<sup>-1</sup> m<sup>-2</sup>): A) Z-Average B) PDI



Código de campo cambiado

Figure 10. Influence of DP/CP ratio on Encapsulation efficiency and Drug Loading of Dexamethasone encapsulated in PLGA-PEG nanoparticles produced by membrane-assisted nanoprecipitation.

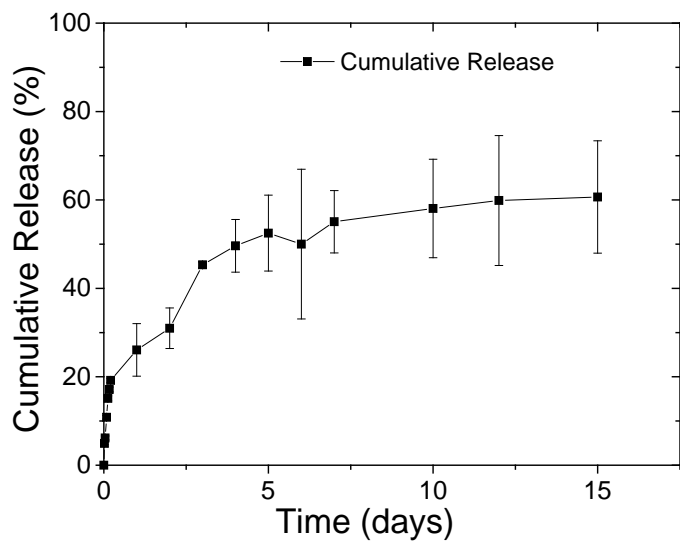


Figure 11. Dexamethasone release from PLGA-PEG nanoparticles produced by membrane-assisted nanoprecipitation.

Table 1. Interpretation of  $R^2$  values and rate constants of dexamethasone release kinetics of PLGA-PEG nanoparticles

<b>Model</b>	<b>Release constant (K)</b>	<b>Release exponent (n)</b>	<b>Regression coefficient (<math>R^2</math>)</b>
Zero Order	3.99	-	0.73
First Order	0.06	-	0.53
Korsmeyer-Peppas	0.47	0.31	0.97
Higuchi	0.32	-	0.87